Report

Cell Reports

A Subtype of Inhibitory Interneuron with Intrinsic Persistent Activity in Human and Monkey Neocortex

Graphical Abstract

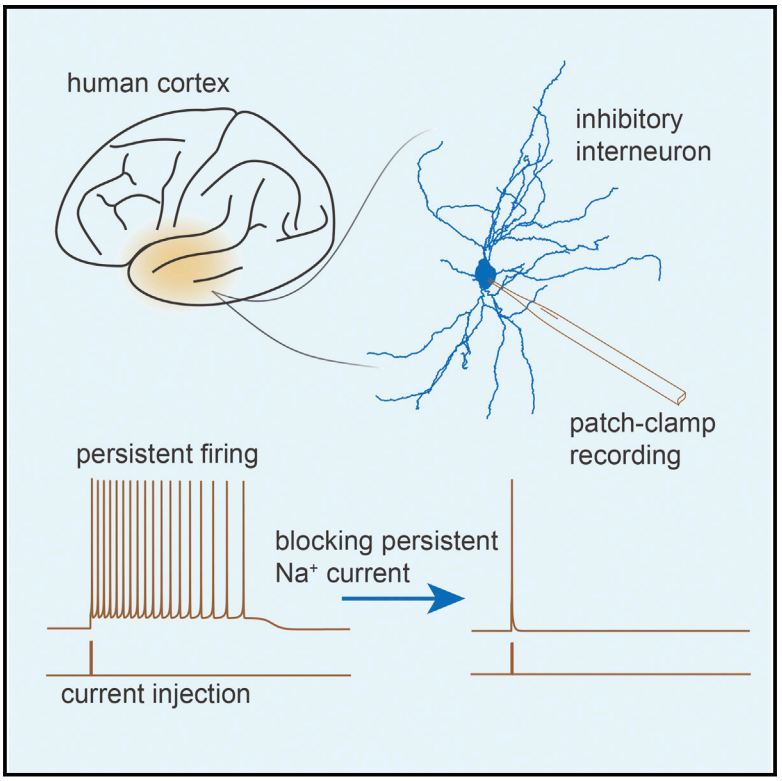

Authors

Bo Wang, Luping Yin, ..., Si Wu, Yousheng Shu

Correspondence

yousheng@bnu.edu.cn

In Brief

A critical step in understanding human cognition is to identify neocortical neuronal types. Here, Wang et al. reveal a subpopulation of human inhibitory interneurons with weak-stimulation-triggered intrinsic persistent activity. This type of neuron is present in primate but not rat neocortex, possibly participating in higher-order brain functions.

Highlights

- Single AP triggers persistent activity in a subset of human cortical interneurons
- The persistent activity is inhibited by strong AP burst
- Neurons with persistent activity exist in primate but not rodent cortex
- The persistent activity is mediated by a persistent Na^+ current

Wang et al., 2015, Cell Reports *10*, 1450–1458
March 10, 2015
http://dx.doi.org/10.1016/j.celrep.2015.02.018

OPEN ACCESS
CellPress

Cell Reports
Report

A Subtype of Inhibitory Interneuron with Intrinsic Persistent Activity in Human and Monkey Neocortex

Bo Wang,[1] Luping Yin,[1] Xiaolong Zou,[2] Min Ye,[3] Yaping Liu,[2] Ting He,[2] Suixin Deng,[2] Yanbo Jiang,[1] Rui Zheng,[1] Yun Wang,[3] Mingpo Yang,[1] Haidong Lu,[2] Si Wu,[2] and Yousheng Shu[2,*]

[1]Institute of Neuroscience and State Key Laboratory of Neuroscience, Shanghai Institutes for Biological Sciences, Chinese Academy of Sciences and University of Chinese Academy of Sciences, Shanghai 200031, China

[2]State Key Laboratory of Cognitive Neuroscience and Learning and IDG/McGovern Institute for Brain Research, School of Brain and Cognitive Sciences, Beijing Normal University, Beijing 100875, China

[3]School of Ophthalmology and Optometry and Eye Hospital, Wenzhou Medical University, Wenzhou 325003, China

*Correspondence: yousheng@bnu.edu.cn

http://dx.doi.org/10.1016/j.celrep.2015.02.018

SUMMARY

A critical step in understanding the neural basis of human cognitive functions is to identify neuronal types in the neocortex. In this study, we performed whole-cell recording from human cortical slices and found a distinct subpopulation of neurons with intrinsic persistent activity that could be triggered by single action potentials (APs) but terminated by bursts of APs. This persistent activity was associated with a depolarizing plateau potential induced by the activation of a persistent Na^+ current. Single-cell RT-PCR revealed that these neurons were inhibitory interneurons. This type of neuron was found in different cortical regions, including temporal, frontal, occipital, and parietal cortices in human and also in frontal and temporal lobes of nonhuman primate but not in rat cortical tissues, suggesting that it could be unique to primates. The characteristic persistent activity in these inhibitory interneurons may contribute to the regulation of pyramidal cell activity and participate in cortical processing.

INTRODUCTION

Individual neurons in the central nervous system evaluate synaptic inputs and transform them into the main output signal, the action potential (AP), following a computational function mainly determined by their electrical properties and morphological features. A huge diversity of neuronal types in the neocortex forms neural circuits that mediate higher order cognitive manifestations. In addition to the great expansion of cortical volume during evolution, unique cell types in the human neocortex may contribute to its versatile mental abilities. For example, the Von Economo neurons (VENs) with distinct morphological characters have only been found in large-brained mammals, including human and nonhuman primates (Economo and Parker, 1929; Evrard et al., 2012; Nimchinsky et al., 1999). This specialized cell type may contribute to the rapid transmission of social information and self-awareness (Allman et al., 2005; Seeley et al., 2006). Except for the finding of VENs, the search for unique cell types in the human neocortex turns out to be unfruitful.

Traditionally, neocortical neurons are considered as "Platonic" or "ideal" devices (Llinás, 1988): their AP firing is limited to the instant when a threshold is reached by cumulative or coincident synaptic inputs (Stuart et al., 1997). Such strict input-output coupling is especially important for the inhibitory interneuron (Galarreta and Hestrin, 2001; Hu et al., 2010), which should provide precise inhibition to maintain network stability (Shu et al., 2003) and facilitate fast and reliable information processing (Cardin et al., 2009; Pouille and Scanziani, 2001). However, the intrinsic properties of neurons are not always "ideal." For example, semilunar granule cells in the dentate gyrus can fire APs for a long duration in response to brief stimulation of the perforant pathway (Larimer and Strowbridge, 2010), and neocortical pyramidal cells (PCs) can generate graded persistent activity while metabotropic receptors are activated (Egorov et al., 2002; Sidiropoulou et al., 2009). Despite the lack of substantial evidence for the behavioral relevance of "unideal" neurons, theoretical studies have suggested important roles of these neurons in cortical functions (Lisman et al., 1998; Loewenstein and Sompolinsky, 2003).

Here we sought to investigate whether human neocortical neurons possess distinct physiological properties. We performed whole-cell recording from neocortical neurons in brain tissues removed from human patients, along with healthy macaque monkeys and rats. We examined the electrophysiological properties and morphological parameters of different types of cortical neurons. We found a subpopulation of human and monkey cortical interneurons that generates intrinsic persistent firing after a brief stimulation, resulting from the activation of persistent Na^+ currents.

RESULTS

Persistent Activity Can Be Triggered by Single APs

In a subpopulation of neurons examined in human slices, we found that single APs evoked by brief (0.5 ~ 2 ms) current pulses triggered persistent firing, i.e., persistent activity, when the V_m was maintained just below the firing threshold (Figures 1A–1C).

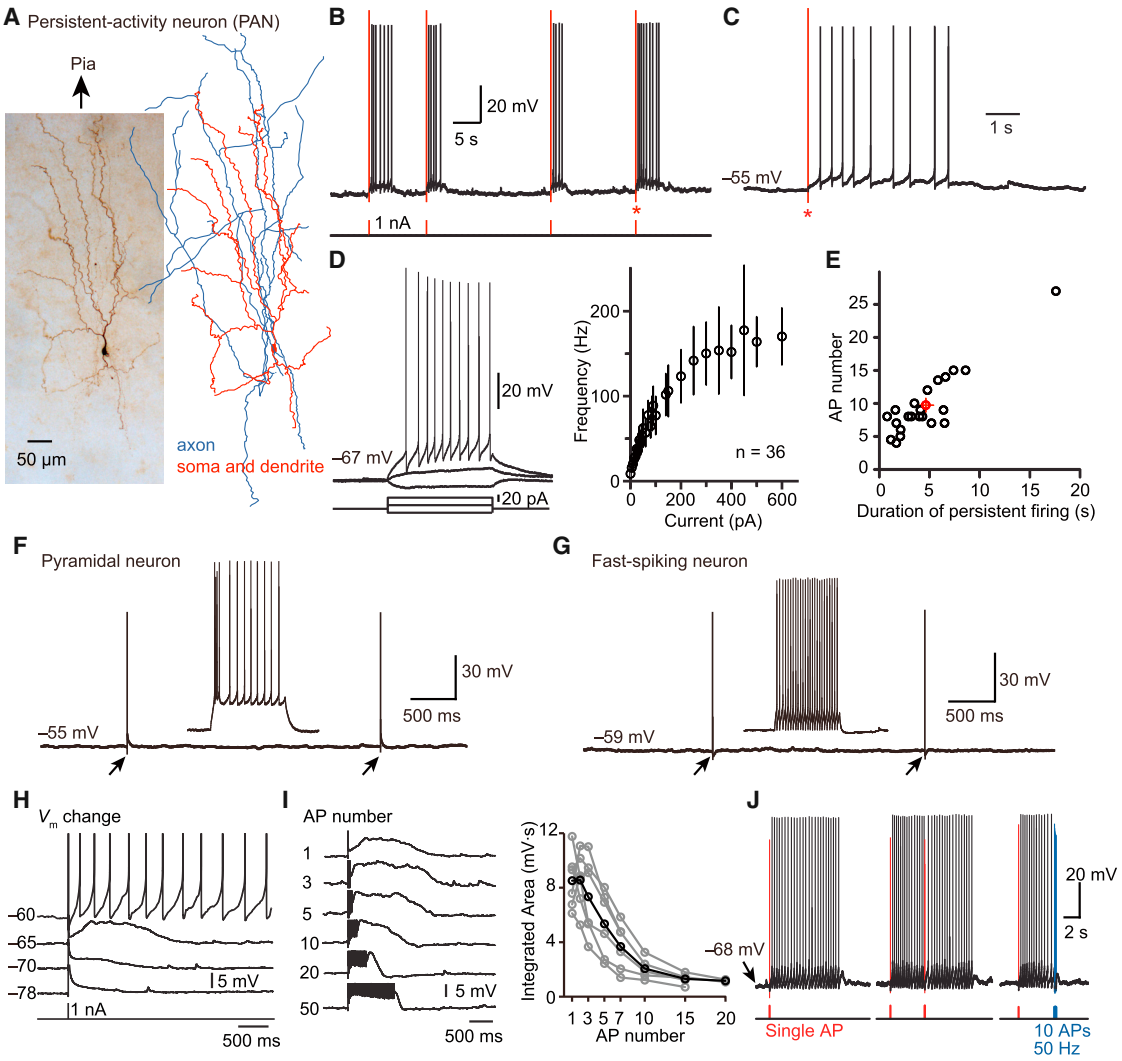

Figure 1. Single APs Trigger Persistent Activity in a Subpopulation of Human Cortical Neurons

(A) DAB staining (left) and reconstruction (right) of a recorded neuron. Blue, axon; red, soma and dendrites.

(B) Example recording from the neuron shown in (A). Note that brief (2-ms) current injections elicited persistent firing.

(C) The expansion of a segment in (B) (asterisk).

(D) (Left) V_m responses of a PAN to 500-ms current pulses. (Right) f-I plot of PANs. Error bars represent SEM.

(E) Scatter plot of the AP number and the duration of persistent firing.

(F and G) Single APs could not trigger persistent activity in PC (F) and FS cells (G). Arrows indicate the brief stimulations. (Insets) Firing patterns of the two cells in response to 500-ms current steps.

(H) Hyperpolarization revealed a depolarizing plateau potential and its dependence on V_m levels.

(I) Progressive reduction in plateau potential with increasing AP number in a 50-Hz burst. (Right) group data showing the dependence of the integrated voltage area of plateau potential on AP number. Grey, individual cells; black, the average.

(J) A burst of APs (but not single AP) could terminate the persistent activity.

The somata of these persistent-activity neurons (PANs) were not pyramid shaped, suggesting that they might represent a subtype of interneuron in the human cortex. To ascertain what proportion of interneurons are PANs, in a subset of experiments, we preferentially sampled from non-PCs (see Experimental Procedures) and found that 9.1% (n = 5 of 55) of them were PANs. In all of the following experiments, we specifically searched for PANs, not only preferentially targeting non-PCs but also discarding most non-PANs, across cortical layers (from layer II to layer V) to investigate their various electrophysiological and morphological properties. PANs exhibited a high-input resistance (R_{in}, 659 ± 57 MΩ, n = 43) and an accelerating-accommodating firing pattern in response to moderate current injection (Figures 1D, S1A, and S1B). The highest firing frequency in response to 500-ms-long current pulses was 153 ± 8 Hz (n = 36; Figure 1D), while the AP half-width was 0.53 ± 0.02 ms (n = 42), similar to that of other non-fast-spiking (non-FS) non-PCs (0.57 ± 0.02 ms, n = 93, p = 0.47). The evoked persistent activity had average

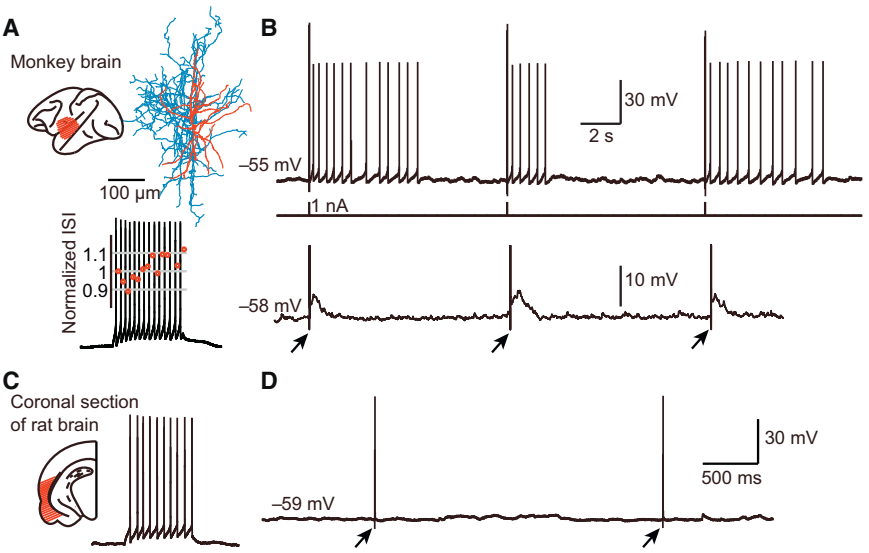

Figure 2. PANs Could Be Found in Monkey but Not Rat Cortex

(A) The sampled area of monkey brain (upper left, sampled area in red shadow) and the reconstruction and firing pattern (below) of a PAN found in monkey cortical slice. (Inset) Normalized interspike interval (ISI).

(B) V_m dependence of the persistent activity and plateau potential in the neuron shown in (A).

(C) The recording area of rat cortical slice (left, in red shadow) and the firing pattern of a rat cortical low-threshold spiking neuron.

(D) Single APs could not trigger plateau potential and any additional APs. Arrows indicate the brief current pulse stimulations.

duration and frequency of 4.6 ± 0.8 s and 2.8 ± 0.4 Hz (Figure 1E), respectively. Similar brief stimulation could trigger single APs but no additional discharges in PCs (n = 24; Figure 1F), fast-spiking (FS) neurons (n = 98; Figure 1G), other non-FS non-PCs (n = 103), and some undefined neurons (n = 80).

A depolarizing plateau potential was found underlying the persistent activity when we injected hyperpolarizing currents small enough to prevent AP generation (Figure 1H). Further hyperpolarization of the membrane potential (V_m) progressively reduced the duration and the amplitude of the plateau potential (Figure 1H). The integrated voltage area was reduced from 4.4 ± 1.1 to 2.1 ± 0.4 mV • s (n = 4), as the V_m hyperpolarized from −65 to −70 mV.

Other forms of intrinsic persistent activity in the cortex normally require a high-frequency burst of APs evoked by prolonged stimulation (Fransén et al., 2006; Sheffield et al., 2011). We therefore examined the dependence on stimulation intensity. Increasing the AP number in a 50-Hz burst progressively reduced the duration and the integrated voltage area of the plateau potential (Figure 1I). The most effective stimuli to "turn on" a plateau potential were 1–3 APs. We next examined whether AP bursts could "turn off" the persistent firing. A brief stimulus identical to the "turn on" stimulus showed no effect on persistent firing. However, bursts with 10 or more APs at 50 Hz could reliably cause an immediate cessation of the persistent firing (Figure 1J).

In total, we collected 68 human PANs. They were from cortical areas, including temporal lobe (n = 61 neurons from 32 patients), frontal lobe (n = 5 from 5 patients), occipital lobe (n = 1), and parietal lobe (n = 1), and patients of different ages (ranging from 3 to 60; <18 years old, n = 13 of 39 patients; Table S1) with either epilepsy (n = 65 from 36 patients) or nonepileptic brain tumor (n = 3 from three patients; Figures S1C–S1E; Table S1). In addition, in cortical slices obtained from two monkeys, we also observed single AP-evoked persistent activity in 7 of 76 non-PCs (Figures 2A and 2B). The occurrence frequency of PANs in non-PCs in monkey tissues (9.2%, n = 7 of 76) was comparable to that in human tissues (9.1%, n = 5 of 55). PANs found in monkey cortical slices behaved similarly and shared similar intrinsic properties with those in human tissues (Figure 2A; Table S2). In cortical slices obtained from rats, however, none of the non-PCs (n = 70 from eight juveniles and n = 118 from five adult rats) showed such persistent activity (Figures 2C and 2D).

PANs Are Inhibitory Interneurons

Following the whole-cell recording, we performed single-cell RT-PCR to further characterize the molecular identity of human PANs (n = 9). All of them expressed glutamic acid decarboxylase I (GAD1 or GAD67), indicating that they were GABAergic neurons. In addition, these neurons expressed at least one of the three markers: somatostatin (SST, n = 5), cholecystokinin (CCK, n = 3), and calretinin (CR) (n = 5) (Figures 3A and 3B), whereas parvalbumin (PV), calbindin (CB), vasoactive intestinal peptide (VIP), or neuropeptide Y (NPY) could not be detected (Figure 3B).

Morphology reconstruction of 27 human PANs revealed that they were located in layers II/III (n = 11), IV (n = 11), and V (n = 5). Among them, 7 were bitufted, 10 bipolar, and 10 multipolar in terms of somatodendritic morphology (Figure S2A). Their dendritic branches were simple, short and vertically oriented, while axonal arbors were intracolumnar and also vertically oriented (Figures 3C and 3D). Sholl analysis showed that axons were more extended and more complex than dendrites (Figure 3D), but never projected to the white matter, which is consistent with features of cortical interneurons. Detailed morphological parameters were presented in Table S3.

PANs Possess Distinct Intrinsic Properties

We next examined the intrinsic membrane properties of human PANs. Since PANs composed of subgroups according to their general descriptive morphologies, layer location, and somatodendritic shape (Figure S2; Table S3), we first examined the intrinsic physiological variations between PAN subgroups. Physiological difference between PANs in different layers only lay in membrane capacitance (C_m; Figure S2B). Bipolar PANs differed from the other two groups by expressing a lower R_{in} and a lower AP threshold (Figure S2C).

To further characterize the intrinsic properties of PANs beyond the variations within the population, we performed clustering

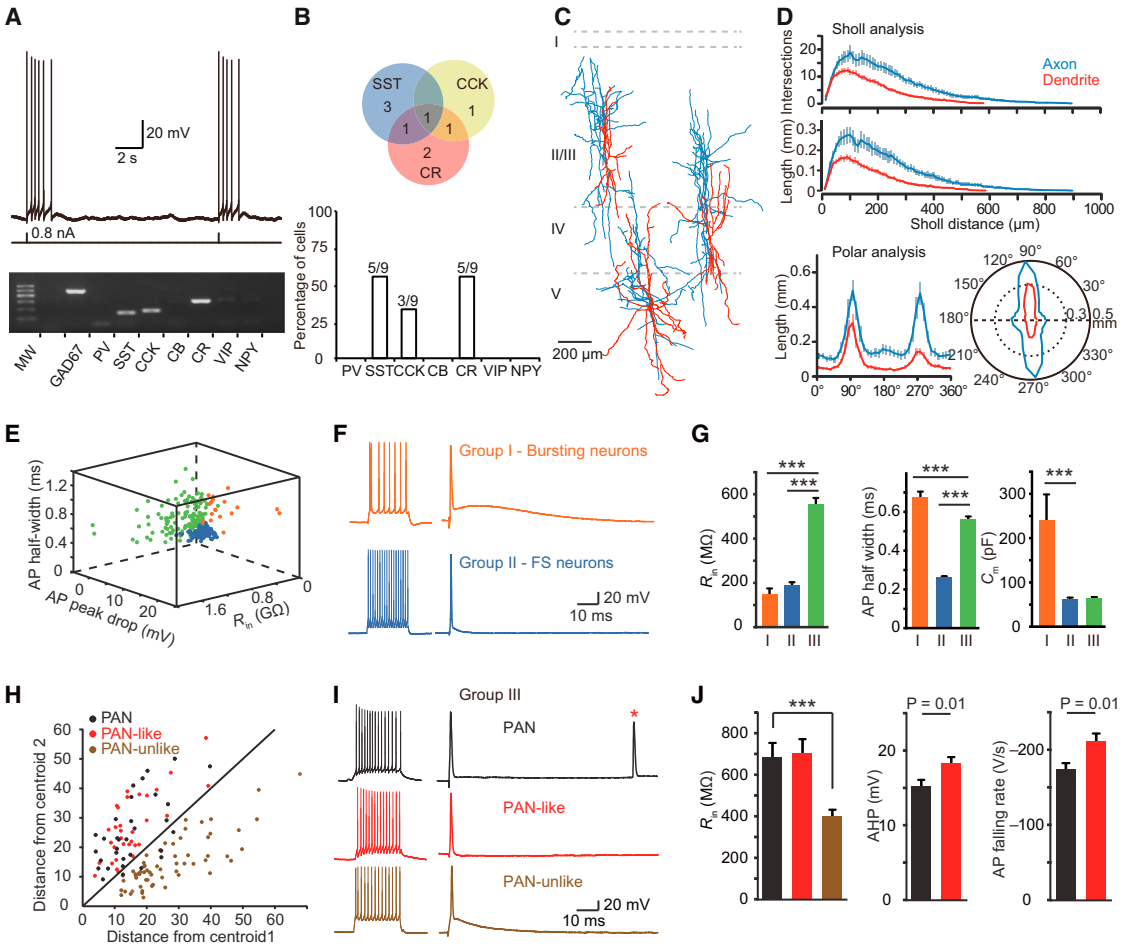

Figure 3. PANs Are Inhibitory Interneurons Possessing Distinct Intrinsic Properties

(A) Example V_m trace (top) and RT-PCR result (bottom) showing that this PAN expressed GAD67, SST, CCK, and CR. Baseline V_m, −62 mV.

(B) Summary of RT-PCR results.

(C) Three example PAN reconstructions (from different slices).

(D) (Upper) Sholl analysis showing that axons were more complex than dendrites. Bin size, 10 μm. (Below) Polar analysis showing that both axonal and dendritic segments were vertically oriented. Bin size, 10°.

(E) Three-dimensional plot of R_{in}, AP peak drop and AP half-width of human non-PCs. Dots represent individual neurons (groups I, II, III were colored in orange, blue, and green, respectively).

(F) Example V_m traces of groups I and II neurons showing their firing patterns and single AP waveforms.

(G) Statistical comparison of intrinsic properties between three groups.

(H) Two-dimensional plot of the distances from cluster centroids of all group III neurons.

(I) Example repetitive firing traces (left) and single AP waveforms of PAN, PAN-like and PAN-unlike neurons. Red asterisk indicates additional AP without further current injection.

(J) Comparison of intrinsic properties between PAN, PAN-like, and PAN-unlike neurons.

Error bars represent SEM. ***p < 0.005.

analysis using 19 physiological parameters from each of 233 human non-PCs in total, of which 33 were PANs. First we performed hierarchical clustering to assign all the neurons into three groups (Figure 3E). Group I consisted of 21 neurons, expressing the broadest AP and showing burst firing pattern, whereas group II consisted of 86 neurons with the thinnest AP and a non-adapting firing pattern, indicating that they were FS neurons (Figures 3F and 3G).

All the 33 PANs fell into group III, along with 93 neurons without persistent activity. Further k-means clustering classified them into two groups: one including most of the PANs (n = 27 of 33) and 32 non-PANs (named PAN-like neurons, sharing a similar firing pattern with PAN) and the other one including 61 non-PANs (PAN-unlike neurons, expressing regular-spiking firing) and only 6 PANs (Figures 3H and 3I). We found that even though PANs did not possess the smallest cell membrane area (PAN C_m, 72.2 ± 5.6; PAN-like neurons, 50.3 ± 3.9; FS neurons, 62.7 ± 3.1; and PAN-unlike neurons, 67.1 ± 4.2 pF), their R_{in} (686 ± 67 MΩ, n = 33) was much higher than that of FS (109 ± 13 MΩ, n = 86) and PAN-unlike (402 ± 30 MΩ, n = 61). PAN-like cells possessed a

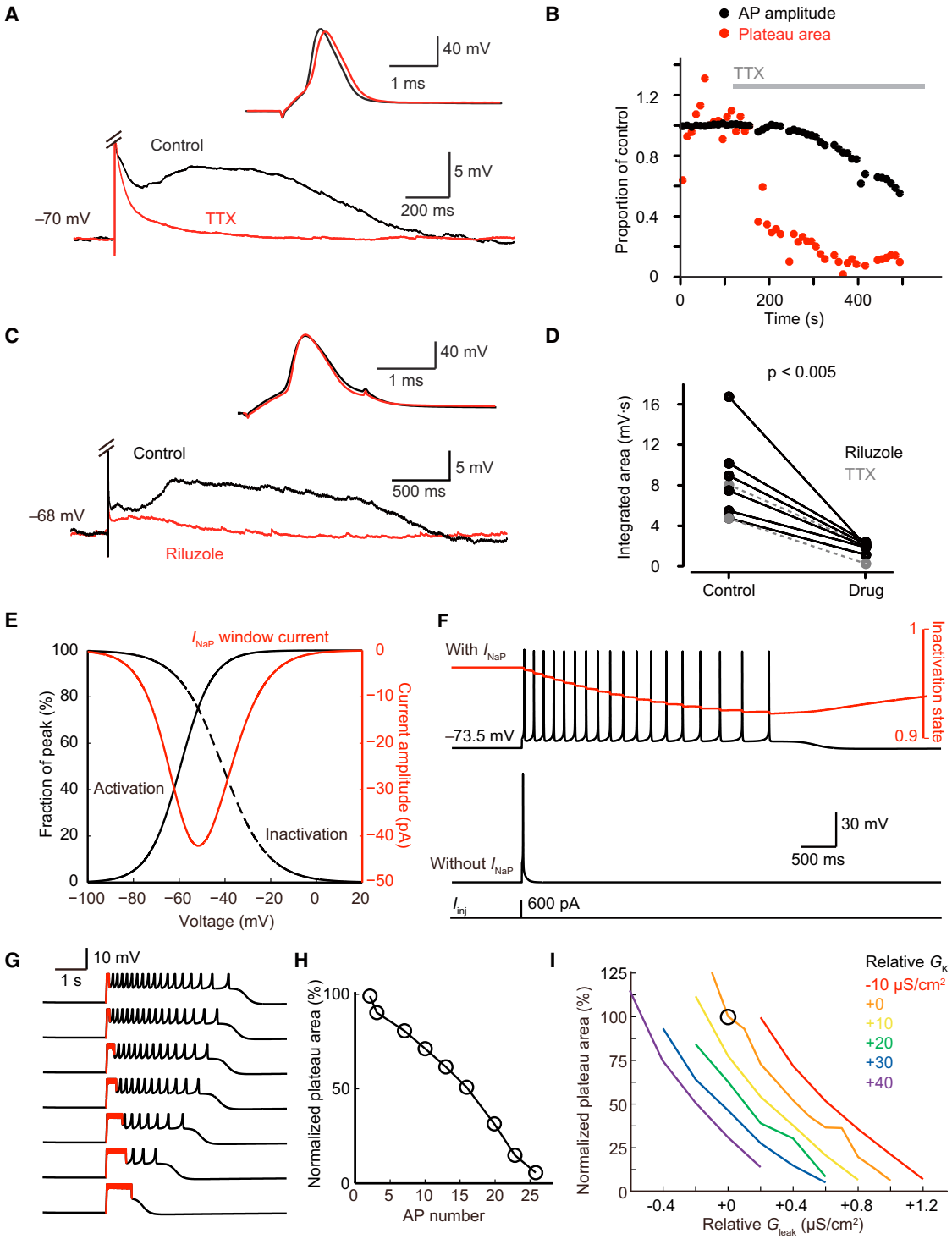

Figure 4. Persistent Na^+ Currents Mediate the Plateau Potential

(A) Overlay of V_m traces in control, and during early periods of TTX application when Na^+-APs still occurred (inset).

(B) Time course of the reduction in AP amplitude and plateau potential area in the cell in (A).

(C) Overlaid traces showing the blockade of plateau potential by application of 20-µM Riluzole.

(D) Group data of Riluzole experiments. The two cells with TTX application were also added, but not included for comparison.

(E–I) Simulation of the generation of persistent activity in PANs. (E) The activation and inactivation curves of I_{NaP} introduced to the single compartment neuron model. The whole-cell window current was also plotted. (F) Persistent activity could be triggered by a 2-ms current pulse in the model neuron with I_{NaP} (upper

(legend continued on next page)

comparable R_{in} (705 ± 66 MΩ, n = 32, p = 0.84) to that of PAN, but exhibited larger AHP (18.2 ± 0.9 versus 15.2 ± 0.8 mV, p = 0.01) and higher maximal AP falling rate (−211 ± 11 versus −174 ± 8 V/s, p < 0.01), suggesting a higher K^+ current density in PAN-like neurons as compared with PANs (Figure 3J; Table S4). In summary, human PANs expressed relatively high R_{in} and low K^+ current density.

Role of Persistent Na^+ Currents

We further investigated the underlying mechanism for the generation of plateau potential in human PANs. Application of fast synaptic transmission blockers (CNQX, 10 μM; DL-APV, 25 μM; and picrotoxin, 50 μM) could not abolish the generation of plateau potential and persistent firing (n = 3), indicating an independence on recurrent synaptic activity. Bath perfusion of tetrodotoxin (TTX) (0.5–1 μM) blocked all APs in 10 min. However, during the first few minutes when effective TTX concentration was low and brief current pulses could still evoke Na^+-APs, the plateau potential was already completely abolished (Figures 4A and 4B), suggesting a role of TTX-sensitive Na^+ currents in mediating the plateau potential. In the presence of Riluzole (20 μM), an inhibitor of persistent Na^+ currents, only the plateau potential was largely attenuated (Figure 4C). The integrated voltage area of the plateau potential was reduced by 76% ± 7% (n = 6; Figure 4D). These results demonstrate a critical role of persistent Na^+ currents in generating the plateau potential, and thus the persistent activity.

In comparison with traditional artificial cerebrospinal fluid (ACSF), the modified ACSF used in this study had a lower level of divalent cations, Ca^{2+} and Mg^{2+} (see Experimental Procedures). Increasing the extracellular Mg^{2+} from 1 to 2 mM caused negligible change in the plateau potential area (by −2.0% ± 7.0%, p = 0.25, n = 5), whereas increasing Ca^{2+} from 1 to 2 mM resulted in significant reduction (by −50.5% ± 6.3%, p < 0.01, n = 6; Figure S3). This result demonstrates that the plateau potential can be modulated by extracellular Ca^{2+} level, consistent with the modulation of persistent Na^+ currents by extracellular Ca^{2+} (Su et al., 2001).

The persistent Na^+ currents are widely expressed in different types of neurons and mediated by the same voltage-gated Na^+ channels responsible for the transient Na^+ current, but they are generally small (Mantegazza et al., 2005; Maurice et al., 2001; Puopolo et al., 2007). The greater R_{in} and lower K^+ current density in PANs may boost V_m depolarization induced by small persistent Na^+ currents.

Single-Compartment Model of PANs

Next we implemented a simplified model using NEURON simulation environment to further investigate the mechanism underlying the generation of persistent activity. In addition to classical Hodgkin-Huxley Na^+ and K^+ channels, we introduced a slowly inactivating persistent Na^+ current (I_{NaP}; Figure 4E) to a single compartment model with the membrane conductance and capacitance proximate to our experimental data. Although the maximal persistent Na^+ conductance was much less than transient conductance (G_{NaP}: G_{NaT} = 1: 1400), they could generate enough window currents (Figure 4E) to depolarize the V_m and cause persistent firing after a single-AP stimulation (Figure 4F). The spontaneous cessation of persistent activity was attributable to cumulative inactivation of the I_{NaP} (Figure 4F). Because repetitive firing facilitates inactivation of I_{NaP}, increasing the number of high-frequency APs by prolonging the stimulation current pulse progressively reduced the duration of plateau potential (Figures 4G and 4H), consistent with the experimental results (Figure 1I).

Experimental results suggested that the high R_{in} and low K^+ current density of PANs may promote the generation of persistent activity. Indeed, elevation of either leaky conductance (i.e., decrease in R_{in}), K^+ conductance (G_K), or both could reduce the integrated area of the plateau potential evoked by single APs (Figure 4I). These modeling results indicate that the activation of I_{NaP}, with the involvement of high R_{in} and low G_K density, is sufficient to generate persistent activity in PANs.

DISCUSSION

We identified a subpopulation of human neocortical inhibitory interneurons that could generate persistent AP firing after a brief stimulation, but ceased firing after a strong stimulation. Experiments and simulations revealed a role of persistent Na^+ current in the generation of persistent activity. Among all cortical interneurons, the estimated percentage of PANs was relatively high (~9% in human and monkey), suggesting that they may play an important role in high-order brain functions.

Most of the PANs were from patients suffering intractable epileptic seizures. The three PANs found in tumor patients without epilepsy suggest that homeostatic changes in epileptic tissues may not be essential for the generation of persistent activity. Additional confirmation came from the similar proportion of PANs in the monkey neocortex. Previous findings demonstrated that the persistent Na^+ current could be altered in the epileptic brain (Stafstrom, 2007), and K^+ currents could be changed and facilitated ictal-like events induced in vitro (Andreasen and Nedergaard, 2012). Because of the lack of healthy human tissues, it is difficult to provide substantial evidence to exclude the possible link between PAN and pathological changes.

We found no such PAN in either juvenile or adult rats, suggesting that they could be unique to primates. However, whether these interneurons exist in other species remains to be further examined. One explanation for the absence of PAN in rat brain could be the lack of high-R_{in} neurons. However, by comparing

trace), but not after removal of I_{NaP} (lower trace). Red line indicates the time course of I_{NaP} inactivation (Q value, see Supplemental Experimental Procedures) during the persistent firing. (G) Example traces showing progressive reduction in plateau potential with increasing stimulation intensity. APs were truncated. Stimulation period in red. (H) Plot of the normalized plateau potential area as a function of the AP number during stimulation. (I) Dependence of the integrated plateau area on membrane leaky conductance (G_{leak}) and voltage-gated K^+ conductance (G_K). The open circle indicates the values used in our model. The colored values and the x-axis values are relative amount of G_K and G_{leak} to the circled values.

the R_{in} distribution between species, we found a comparable proportion of high-resistance neurons between human and rat (Figure S4A). There were indeed rat neurons with as high resistance as PANs. Moreover, PANs occupied the lowest conductance density ($1/R_{in}C_m$) fraction of human non-PCs, and the rat neurons had relatively high conductance density (Figure S4B). The difference in distribution of membrane conductance density between human and rat could partially explain why PAN was not found in rat brain. However, many other factors might also be involved, including Na^+ channel kinetics and other membrane channels, which are yet to be investigated.

Our experimental and modeling results indicate that persistent activity of PANs is attributed to the activation of persistent Na^+ currents. Previous studies revealed important contribution of this current to spontaneous pace-making activities (Khaliq and Bean, 2010; Puopolo et al., 2007). However, single AP-triggered sustained activation of the persistent Na^+ current has not been reported elsewhere, possibly because various K^+ currents are counteracting its depolarizing effect (Hage and Salkoff, 2012; Stafstrom et al., 1985) and the persistent Na^+ current is normally too small to maintain V_m depolarization. The generation of persistent activity in PANs is also attributable to their unique intrinsic properties. Modeling results further demonstrate that higher R_{in} and lower K^+ current can facilitate the sustained depolarization by persistent Na^+ currents. A high-frequency AP burst can induce severe inactivation of the persistent Na^+ current (Fleidervish and Gutnick, 1996) and consequently "turn off" the persistent activity. The persistent Na^+ current is also modulated by extracellular Ca^{2+} concentration (Su et al., 2001). Increasing the extracellular Ca^{2+} concentration decreased the plateau potential. The Ca^{2+} concentration (1 mM) in modified ACSF is lower than that in normal ACSF (2 mM), but has been reported to better mimic the physiological conditions (Harris et al., 1984; Zhang et al., 1990) and facilitate in vivo-like network activity (Sanchez-Vives and McCormick, 2000). Considering that Ca^{2+} concentration in the CSF varies when cortical activity changes (Massimini and Amzica, 2001; Torres et al., 2012), we speculate that the persistent activity in PANs may dynamically participate in different cortical states.

Similar to the delay-period activity during working memory (Goldman-Rakic, 1995) and the activity induced pharmacologically in cortical PCs (Egorov et al., 2002; Sidiropoulou et al., 2009), persistent activity found in human and monkey cortical interneurons could be a putative substrate responsible for the storage of a transient memory trace or the modulation of persistent activity in principle neurons. In addition, PANs provide a paradoxical cortical inhibition: in response to weak synaptic inputs, these neurons generate persistent firing, elevate cortical inhibition, and decrease the gain of neural circuit; in contrast, strong inputs hold back excessive firing and cause a reduction in cortical inhibition. Thus, PANs could enhance discrimination between behaviorally relevant and irrelevant cues (Duncan et al., 1997; Easterbrook, 1959) by differentially modulating activity in principal PCs. The tunable inhibition they provide may also contribute to the gain control mechanisms active during sensory processing and attention (Curtis and D'Esposito, 2003; Hillyard et al., 1998; Isaacson and Scanziani, 2011).

EXPERIMENTAL PROCEDURES

Handling and use of the human brain tissue was approved by the Biomedical Research Ethics Committee of Shanghai Institutes for Biological Sciences (license no. ER-SIBS-221004). The use and care of rodents complied with the guidelines of the Animal Advisory Committee at the Shanghai Institutes for Biological Sciences. All procedures regarding monkey experiments were performed in accordance with the NIH Guidelines and were approved by the Institutional Animal Care and Use Committee of Beijing Normal University. A detailed description of the Experimental Procedures is included in the Supplemental Experimental Procedures.

Electrophysiological Recording

Human neocortical tissues obtained were surgically removed to cure intractable epilepsy or brain tumor (Table S1). Monkey neocortical tissues were obtained from the temporal and frontal lobes of two adult macaque monkeys during deep general anesthesia. Slices with a thickness of 250–300 μm were cut in the ice-cold sucrose-ACSF from cortical tissues with clear white and gray matter and incubated at 34.5°C in a normal ACSF for about 40 min and then room temperature until use. Coronal slices of rat frontal or temporal cortex were prepared from both juvenile and adult Sprague-Dawley rats in the same way to that of human slices. We recorded neurons in the entorhinal, temporal association, and also auditory cortex of rats and also in the medial prefrontal cortex of juveniles.

During recordings, slices were perfused with modified ACSF (modified from normal ACSF; in mM: 3.5 KCl, 1 $CaCl_2$, and 1 $MgSO_4$) at 35°C–36°C. Whole-cell recordings were achieved using glass pipettes filled with K-gluconate-based solution. We recorded the V_m responses to serials of hyperpolarizing and depolarizing current steps (500 ms in duration) and examined the passive and active intrinsic properties. Brief current pulses (0.5–2.0 ms in duration, 0.5–2.0 nA in amplitude) were injected into each neuron to evoke single APs. PANs were identified by their ability to reliably generate long-lasting firing or depolarizing plateau potential (>500 ms in duration) after single-AP stimulation. Liquid junction potential (~15 mV) was not corrected.

To ascertain what proportion of inhibitory neurons are PANs, in a subset of experiments, we preferentially sampled from non-PCs without any intentional bias toward particular subtypes of them. We visually avoided pyramid-shaped neurons under DIC microscope and targeted all other neurons from cortical layer II to layer V. After recording, the recorded neurons were re-examined by 3,3′-diaminobenzidine tetrahydrochloride (DAB) staining or filled fluorescent dye, and PCs were further ruled out. In order to efficiently catch PANs in other experiments (not for proportion estimation), we specifically searched for PANs in non-PCs and discarded most non-PAN recordings.

Morphology Reconstruction

After electrophysiological recording, slices were fixed and stained with DAB using a standard ABC protocol. Three-dimensional reconstructions were then performed in the stained neurons using the Neurolucida system. The reconstructed cells without obvious cutoff of main process were selected for anatomical analysis.

Single-Cell RT-PCR

We performed single-cell RT-PCR experiments using a well-established protocol, but with minor modifications (see Supplemental Experimental Procedures). A multiplex PCR was performed for each recording, followed by PCR reactions each for a specific gene. All the primers were tested to be effective without obvious unintended amplification in multiplex PCR using total human brain RNA as a template before single-cell experiments.

NEURON Model

We implemented a single compartment model, using NEURON 7.3, with transient voltage-gated Na^+ and "delayed-rectifier" K^+ currents responsible for AP generation, leaky currents, and persistent Na^+ currents. The leaky conductance and membrane capacitance were set close to experimental data.

Statistical Analysis

All of the electrophysiological and morphological values were presented as mean ± SEM. Statistical significance of difference was tested using Student's t test. Passive parameters were derived from V_m responses (<10-mV deflection from resting potential) to hyperpolarizing current steps. AP parameters were derived from V_m responses to threshold current steps. Clustering analysis and principle component analysis were performed using MATLAB. Both the hierarchical clustering and k-means clustering were performed using calculated Euclidean distance.

SUPPLEMENTAL INFORMATION

Supplemental Information includes Supplemental Experimental Procedures, four figures, and four tables and can be found with this article online at http://dx.doi.org/10.1016/j.celrep.2015.02.018.

AUTHOR CONTRIBUTIONS

B.W., L.Y., Y.L., T.H., S.D., Y.J., and R.Z. performed electrophysiological recordings. B.W. performed single-cell RT-PCR experiments. M.Y. and B.W. reconstructed the recorded cells. X.Z., B.W., and S.W. performed simulations. H.L. helped with the monkey experiments. Y.W., M.P.Y., and Y.S. helped with data analysis. B.W., Y.W., and Y.S. designed the experiments and wrote the paper.

ACKNOWLEDGMENTS

This work was supported by the National Natural Science Foundation of China Project (31430038 and 31025012) and the 973 Program (2011CBA00400). We thank Dr. Udo Kraushaar for his valuable comments.

Received: May 1, 2014
Revised: December 2, 2014
Accepted: February 2, 2015
Published: March 5, 2015

REFERENCES

Allman, J.M., Watson, K.K., Tetreault, N.A., and Hakeem, A.Y. (2005). Intuition and autism: a possible role for Von Economo neurons. Trends Cogn. Sci. *9*, 367–373.

Andreasen, M., and Nedergaard, S. (2012). Heterogeneous firing behavior during ictal-like epileptiform activity in vitro. J. Neurophysiol. *107*, 1379–1392.

Cardin, J.A., Carlén, M., Meletis, K., Knoblich, U., Zhang, F., Deisseroth, K., Tsai, L.H., and Moore, C.I. (2009). Driving fast-spiking cells induces gamma rhythm and controls sensory responses. Nature *459*, 663–667.

Curtis, C.E., and D'Esposito, M. (2003). Persistent activity in the prefrontal cortex during working memory. Trends Cogn. Sci. *7*, 415–423.

Duncan, J., Humphreys, G., and Ward, R. (1997). Competitive brain activity in visual attention. Curr. Opin. Neurobiol. *7*, 255–261.

Easterbrook, J.A. (1959). The effect of emotion on cue utilization and the organization of behavior. Psychol. Rev. *66*, 183–201.

Economo, C., and Parker, S. (1929). The Cytoarchitectonics of the Human Cerebral Cortex (London: Humphrey Milford, Oxford University Press).

Egorov, A.V., Hamam, B.N., Fransén, E., Hasselmo, M.E., and Alonso, A.A. (2002). Graded persistent activity in entorhinal cortex neurons. Nature *420*, 173–178.

Evrard, H.C., Forro, T., and Logothetis, N.K. (2012). Von Economo neurons in the anterior insula of the macaque monkey. Neuron *74*, 482–489.

Fleidervish, I.A., and Gutnick, M.J. (1996). Kinetics of slow inactivation of persistent sodium current in layer V neurons of mouse neocortical slices. J. Neurophysiol. *76*, 2125–2130.

Fransén, E., Tahvildari, B., Egorov, A.V., Hasselmo, M.E., and Alonso, A.A. (2006). Mechanism of graded persistent cellular activity of entorhinal cortex layer v neurons. Neuron *49*, 735–746.

Galarreta, M., and Hestrin, S. (2001). Spike transmission and synchrony detection in networks of GABAergic interneurons. Science *292*, 2295–2299.

Goldman-Rakic, P.S. (1995). Cellular basis of working memory. Neuron *14*, 477–485.

Hage, T.A., and Salkoff, L. (2012). Sodium-activated potassium channels are functionally coupled to persistent sodium currents. J. Neurosci. *32*, 2714–2721.

Harris, R.J., Wieloch, T., Symon, L., and Siesjö, B.K. (1984). Cerebral extracellular calcium activity in severe hypoglycemia: relation to extracellular potassium and energy state. J. Cereb. Blood Flow Metab. *4*, 187–193.

Hillyard, S.A., Vogel, E.K., and Luck, S.J. (1998). Sensory gain control (amplification) as a mechanism of selective attention: electrophysiological and neuroimaging evidence. Philos. Trans. R. Soc. Lond. B Biol. Sci. *353*, 1257–1270.

Hu, H., Martina, M., and Jonas, P. (2010). Dendritic mechanisms underlying rapid synaptic activation of fast-spiking hippocampal interneurons. Science *327*, 52–58.

Isaacson, J.S., and Scanziani, M. (2011). How inhibition shapes cortical activity. Neuron *72*, 231–243.

Khaliq, Z.M., and Bean, B.P. (2010). Pacemaking in dopaminergic ventral tegmental area neurons: depolarizing drive from background and voltage-dependent sodium conductances. J. Neurosci. *30*, 7401–7413.

Larimer, P., and Strowbridge, B.W. (2010). Representing information in cell assemblies: persistent activity mediated by semilunar granule cells. Nat. Neurosci. *13*, 213–222.

Lisman, J.E., Fellous, J.M., and Wang, X.J. (1998). A role for NMDA-receptor channels in working memory. Nat. Neurosci. *1*, 273–275.

Llinás, R.R. (1988). The intrinsic electrophysiological properties of mammalian neurons: insights into central nervous system function. Science *242*, 1654–1664.

Loewenstein, Y., and Sompolinsky, H. (2003). Temporal integration by calcium dynamics in a model neuron. Nat. Neurosci. *6*, 961–967.

Mantegazza, M., Yu, F.H., Powell, A.J., Clare, J.J., Catterall, W.A., and Scheuer, T. (2005). Molecular determinants for modulation of persistent sodium current by G-protein betagamma subunits. J. Neurosci. *25*, 3341–3349.

Massimini, M., and Amzica, F. (2001). Extracellular calcium fluctuations and intracellular potentials in the cortex during the slow sleep oscillation. J. Neurophysiol. *85*, 1346–1350.

Maurice, N., Tkatch, T., Meisler, M., Sprunger, L.K., and Surmeier, D.J. (2001). D1/D5 dopamine receptor activation differentially modulates rapidly inactivating and persistent sodium currents in prefrontal cortex pyramidal neurons. J. Neurosci. *21*, 2268–2277.

Nimchinsky, E.A., Gilissen, E., Allman, J.M., Perl, D.P., Erwin, J.M., and Hof, P.R. (1999). A neuronal morphologic type unique to humans and great apes. Proc. Natl. Acad. Sci. USA *96*, 5268–5273.

Pouille, F., and Scanziani, M. (2001). Enforcement of temporal fidelity in pyramidal cells by somatic feed-forward inhibition. Science *293*, 1159–1163.

Puopolo, M., Raviola, E., and Bean, B.P. (2007). Roles of subthreshold calcium current and sodium current in spontaneous firing of mouse midbrain dopamine neurons. J. Neurosci. *27*, 645–656.

Sanchez-Vives, M.V., and McCormick, D.A. (2000). Cellular and network mechanisms of rhythmic recurrent activity in neocortex. Nat. Neurosci. *3*, 1027–1034.

Seeley, W.W., Carlin, D.A., Allman, J.M., Macedo, M.N., Bush, C., Miller, B.L., and Dearmond, S.J. (2006). Early frontotemporal dementia targets neurons unique to apes and humans. Ann. Neurol. *60*, 660–667.

Sheffield, M.E., Best, T.K., Mensh, B.D., Kath, W.L., and Spruston, N. (2011). Slow integration leads to persistent action potential firing in distal axons of coupled interneurons. Nat. Neurosci. *14*, 200–207.

Shu, Y., Hasenstaub, A., and McCormick, D.A. (2003). Turning on and off recurrent balanced cortical activity. Nature *423*, 288–293.

Sidiropoulou, K., Lu, F.M., Fowler, M.A., Xiao, R., Phillips, C., Ozkan, E.D., Zhu, M.X., White, F.J., and Cooper, D.C. (2009). Dopamine modulates an mGluR5-mediated depolarization underlying prefrontal persistent activity. Nat. Neurosci. *12*, 190–199.

Stafstrom, C.E. (2007). Persistent sodium current and its role in epilepsy. Epilepsy Curr. *7*, 15–22.

Stafstrom, C.E., Schwindt, P.C., Chubb, M.C., and Crill, W.E. (1985). Properties of persistent sodium conductance and calcium conductance of layer V neurons from cat sensorimotor cortex in vitro. J. Neurophysiol. *53*, 153–170.

Stuart, G., Spruston, N., Sakmann, B., and Häusser, M. (1997). Action potential initiation and backpropagation in neurons of the mammalian CNS. Trends Neurosci. *20*, 125–131.

Su, H., Alroy, G., Kirson, E.D., and Yaari, Y. (2001). Extracellular calcium modulates persistent sodium current-dependent burst-firing in hippocampal pyramidal neurons. J. Neurosci. *21*, 4173–4182.

Torres, A., Wang, F., Xu, Q., Fujita, T., Dobrowolski, R., Willecke, K., Takano, T., and Nedergaard, M. (2012). Extracellular Ca^{2+} acts as a mediator of communication from neurons to glia. Sci. Signal. *5*, ra8.

Zhang, E.T., Hansen, A.J., Wieloch, T., and Lauritzen, M. (1990). Influence of MK-801 on brain extracellular calcium and potassium activities in severe hypoglycemia. J. Cereb. Blood Flow Metab. *10*, 136–139.